

Kerr frequency comb generation in fiber Fabry-Pérot resonator: technological locks and leveraging fiber properties

Germain Bourcier^{1,2*}, Safia Mohand Ousaid¹, Stéphane Balac³, Julien Lumeau⁴, Antonin Moreau⁴, Thomas Bunel⁵, Matteo Conforti⁵, Arnaud Mussot⁵, Arnaud Fernandez¹ and Olivier Llopis¹

¹LAAS-CNRS, Université de Toulouse, CNRS, UPS, Toulouse, France

²CNES, 18 avenue Edouard Belin, F-31401 Toulouse, France

³IRMAR, Université de Rennes, CNRS, Campus de Beaulieu, 35042 Rennes, France

⁴Université Aix Marseille, CNRS, Centrale Med, Institut Fresnel, Marseille, France

⁵Université de Lille, CNRS, UMR-8523-PhLAM Physique des Lasers Atomes et Molécules, F-59000, Lille, France

Abstract. We explore fiber Fabry-Pérot (FFP) resonators, a new platform for frequency comb generation. We experimentally identified mirror diffraction losses dependent on the effective area of the fiber and simulated them via Fourier optics. In the nonlinear regime, a linear stability analysis of a generalized Lugiato-Lefever equation revealed optimization of reflectivity and detuning, leading to a significant reduction in the required power threshold for comb generation compared to linear regime, and to improved energy frugality. Furthermore, controlled or exploited birefringence in various experimental settings enabled the generation of Kerr frequency combs and stimulated Brillouin lasers. In this communication we propose an overview of the practical characteristics related to the fabrication and use of these resonators.

1 Introduction

The fiber Fabry-Pérot (FFP) resonator is an innovative platform, as evidenced by the recent enthusiasm surrounding its use, particularly for frequency comb generation [1-3] or stabilization through feedback injection [4]. The FFP consists of a short length of optical fiber with FC-PC connectors onto which high reflectivity (>99.8%) multilayer dielectric mirrors are deposited, with a bandwidth of 40 nm centred at 1.55 μm . The centimetric dimensions of the FFP confer a Free Spectral Range (FSR) in the microwave domain. The low losses associated with propagation in the optical fiber enable achieving high quality factors up to 5.10^9 and taking advantage of fiber nonlinearity. The mirror is the primary source of losses while the level of reflectivity must be precisely controlled. In this paper, we review all the knowledge acquired through our experience on the FFP intended for frequency comb generation.

2 Diffraction loss

The effective area A_{eff} of a fiber impacts its nonlinear coefficient according to the relation $\gamma = 2\pi n_2 / (\lambda A_{eff})$, where λ is the wavelength and n_2 is the nonlinear index. However, resonators realized with low effective area fiber (HNL fiber) feature lower quality factor (Q) than resonators based on multimode fiber (Fig.1.). This behaviour can be explained through losses induced by diffraction. The deposited mirror has a thickness of a few microns, and its surface extends over the entire FC-PC

connector. Therefore, we can consider that the propagation of the reflected beam is not confined within the mirror. Moreover, the smaller the cross-section of the optical guide, the wider the diffraction within the mirror. Upon reflection, a portion of the field is lost in the cladding. The resulting loss is substantial and significantly reduces the performance of the resonators. Fourier optics simulations have confirmed our observations (Fig. 1.).

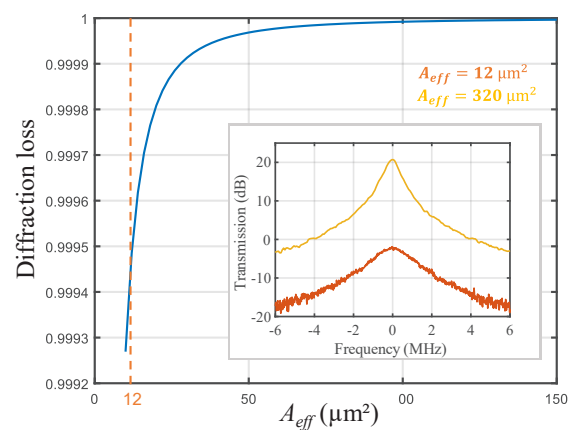


Fig. 1. Fourier optics simulation of losses incurred by the diffraction of a Gaussian beam with an effective area A_{eff} upon reflection in a multilayer mirror a few microns thick. The inset represents the transfert function of two FFPs with $A_{eff} = 12 \mu\text{m}^2$ fiber and $A_{eff} = 320 \mu\text{m}^2$ fiber. The FFP with the smaller fiber area experienced a decrease in transmission and a higher FWHM.

* Corresponding author: gbourcier@laas.fr

3 Modulation instability threshold

After achieving excellent quality factors (in the range of 10^8 or 10^9) through FFP optimization in the linear regime, we focused on the optimization of reflectivity and frequency detuning in the nonlinear regime. We therefore performed a linear stability analysis of a generalized Lugiato-Lefever equation describing the FFP behaviour under continuous pumping, allowing us to get the modulation instability (MI) threshold with respect to pump power as a function of detuning (Fig. 2(a)) and reflectivity. MI is the first stage of comb generation. Our study reveals a value of reflectivity and detuning that minimizes the MI threshold. This optimal reflectivity exceeds what is achieved using a linear model of the cavity maximizing the intracavity power. This change in reflectivity allows for a non-negligible 15.6% reduction in the threshold power. This unexpected outcome can be explained by the fact that linear model optimization maximizes the number of photons in the cavity, but in the nonlinear model, photons lifetime becomes important in their interaction with matter. Therefore, having fewer photons but with a longer lifetime is preferable.

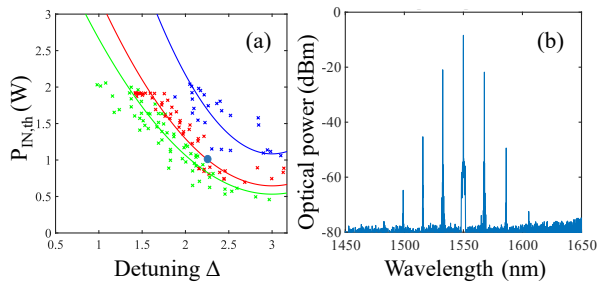


Fig. 2. (a) Intracavity power threshold as a function of normalized detuning for FFPs with different A_{eff} . Solid lines are theory while crosses show experimental data. Red: $12 \mu\text{m}^2$; green: $72 \mu\text{m}^2$; blue: $85 \mu\text{m}^2$. (b) Modulation instability subcomb corresponding to blue point on red curve in (a).

4 Fiber properties

Once the resonator is optimized for Kerr frequency comb generation, several important experimental points remain to be clarified. The first point is the presence of Brillouin effect due to a spectral overlap between Stimulated Brillouin Scattering (SBS) gain and cavity resonances ($\nu_B \approx 10 \text{ GHz}$, $\Delta\nu = 50 \text{ MHz}$). Given that the FFPs have FSRs in the GHz range, it is crucial to precisely adjust the length of the FFP to either avoid SBS or to intensify it to generate with FWM a cascaded Brillouin comb [4]. The second point is optical fiber natural birefringence. In a single-mode fiber FFP, this leads to the coexistence of two families of cavity modes with orthogonal polarizations. We can take advantage of this asymmetry and use the two polarizations as separate channels. This opens up possibilities for various schemes such as stabilization and comb generation [1] or even dual comb generation. Additionally, we manufactured precision mechanical parts to apply pressure or torsion on the fiber. Controlling stress-induced birefringence allows us to modulate the frequency spacing between the two mode families. It

enables us to reach SBS gain in cross-polarizations. Pumping the FFP on one polarization results in a Stimulated Brillouin Laser (SBL) on the other polarization. This SBL is less noisy and more powerful than the pump laser. Our FFP SBL is shown in Fig. 3(a). It can be used for the generation of dispersive Kerr solitons [2] (chaotic comb in Fig. 3(b)). This cross-polarization SBL pumping scheme allows to balance thermo-optical effect to obtain ultra-stable comb sources.

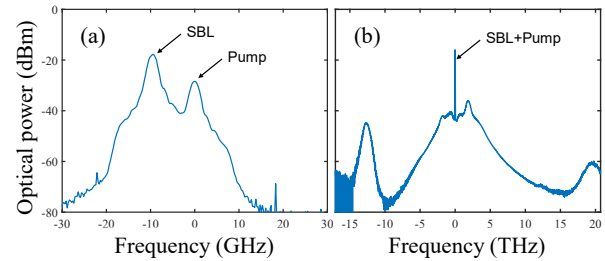


Fig. 3. Experimental optical spectrum of SBL (a) and SBL pumped chaotic comb (b) (20 cm, $A_{eff} = 12 \mu\text{m}^2$).

5 Conclusion

To conclude, we propose a feedback based on our experience in the fabrication and utilization of the fiber Fabry-Pérot resonator. We identify diffraction as a major source of power losses limiting their performance. The FFP enables the generation of frequency combs. The minimum power required for their generation is analytically calculated and experimentally verified. This leads to an optimization of reflectivity and detuning specific to the nonlinear regime. Birefringence in resonators is controlled or utilized for various experimental configurations, including the generation of Stimulated Brillouin. Our finding could be of great interest in all fiber Fabry-Pérot applications that require low losses and low power thresholds, especially for frequency comb generation.

The present research was supported by French Ministry of Armed Forces – Agence de l’Innovation Défense (AID) and the national space center (CNES).

References

1. T. Bunel, M. Conforti, Z. Ziani, J. Lumeau, A. Moreau, A. Fernandez, O. Llopi, G. Bourcier, A. Mussot, *APL Phot.* **9**, 010804 (2024)
2. K. Jia, X. Wang, D. Kwon, J. Wang, E. Tsao, H. Liu, X. Ni, J. Guo, M. Yang, X. Jiang, J. Kim, S. Zhu, Z. Xie, S.-W. Huang, *Phys. Rev. Lett.* **125**, 143902 (2020)
3. T. Bunel, M. Conforti, J. Lumeau, A. Moreau, A. Fernandez, O. Llopi, J. Roul, A. M. Perego, A. Mussot, *CLEO Europe* (2023)
4. S. Mohand Ousaid, G. Bourcier, A. Fernandez, O. Llopi, J. Lumeau, A. Moreau, T. Bunel, M. Conforti, A. Mussot, V. Crozatier, S. Balac, *Opt. Lett.* **49**, 1933-1936 (2024)